
Does trace element composition of bivalve shells record ultra-high frequency environmental variations?

Poitevin Pierre ^{1,2,*}, Chauvaud Laurent ⁶, Pecheyran Christophe ³, Lazure Pascal ⁴, Jolivet Aurélie ⁵,
Thebault Julien ¹

¹ Univ. Brest, CNRS, IRD, Ifremer, LEMAR, F-29280, Plouzané, France

² Fisheries and Oceans Canada, Maurice Lamontagne Institute, Mont-Joli, QC, Canada

³ Laboratoire de Chimie Analytique Bio-inorganique et Environnement, Institut Pluridisciplinaire de Recherche sur L'Environnement et Les Matériaux, CNRS, UMR 5254, Université de Pau et des Pays de L'Adour, Pau, France

⁴ Univ. Brest, CNRS, IRD, UBO, Ifremer, LOPS, F-29280, Plouzané, France

⁵ TBM Environnement/Somme, 2 Rue de Suède, 56400, Auray, France

⁶ Univ. Brest, CNRS, IRD, Ifremer, LEMAR, F-29280, Plouzané, France

* Corresponding author : Pierre Poitevin, email address : poitevin.pierre@gmail.com

laurent.chauvaud@univ-brest.fr ; christophe.pecheyran@univ-pau.fr ; pascal.lazure@ifremer.fr ;
a.jolivet@tbm-environnement.com ; julien.thebault@univ-brest.fr

Abstract :

Saint-Pierre and Miquelon (SPM) is a small archipelago where instrumental measures based on water column velocity and temperature profiles compiled comprehensive evidence for strong near-diurnal (25.8h) current and bottom temperature oscillations (up to 11.5 °C) which is possibly the largest ever observed — at any frequency — on a stratified mid-latitude continental shelf. The main objective of our study was to identify if *Placopecten magellanicus* can record on its shell these high frequency environmental variations. To this end, we have tried to identify proxies for water temperature and food availability through development of a new ultra-high resolution LA-ICPMS analyses method capable of resolving shell surface elemental composition with a 10 µm resolution. This method was applied on two shell fragments, both representing the third year of growth and 2015 annual growth period, respectively coming from two environmentally contrasted sites, more (30 m depth) or less (10 m depth) affected by high frequency thermal oscillations. Our results strongly suggest a relationship between phytoplankton biomass and barium incorporation into *P. magellanicus* shells at both sites. Even if *P. magellanicus* might present a physiological control of magnesium incorporation, the shape of the two Mg/Ca profiles seems to illustrate that temperature also exerts a control on magnesium incorporation in *P. magellanicus* shells from SPM. While U/Ca and Mg/Ca profiles show a strong positive correlation for 30 m site shell, suggesting that uranium incorporation in *P. magellanicus* shell is at least partially temperature dependent. The absence of such correlation for 10 m site shell suggests differences in uranium environmental availability or in *P. magellanicus* biomineralization between these two sites. The resolution of this new analytical method raises questions about such data interpretation related to *P. magellanicus* growth dynamics and physiology or individual scale based environmental measurements.

Highlights

► A new method to resolve shell elemental composition with a 10 μm resolution. ► Ba/Ca of *Placopecten magellanicus* shell seem to be related to phytoplankton dynamic. ► Mg/Ca and U/Ca of *P. magellanicus* shell seem partially temperature dependent. ► This species might also present a physiological control on Mg and U incorporation. ► This method may contribute to a better understanding of ion incorporation in shells.

Keywords : Ultra-high resolution LA-ICPMS, *Placopecten magellanicus*, shell chemistry, trace elements, environmental change, bivalve, environmental proxies, North Atlantic, Saint-Pierre and Miquelon, Coastal Trapped Wave.

59 **1. Introduction**

60 Saint-Pierre and Miquelon (SPM) is a small archipelago at the confluence of major oceanic
61 currents, marking the boundary between the North Atlantic Ocean subtropical and subpolar
62 gyres. However, SPM archipelago hydrodynamics is poorly known and its physic
63 observations (sensor deployments) only began very recently. In this context, instrumental
64 measurements based on water column velocity and temperature profiles compiled
65 comprehensive evidence for strong near-diurnal (25.8h) current and bottom temperature
66 oscillations (up to 11.5°C) from July to October between 10 and 80m depth. This feature is
67 possibly the largest ever observed, at any frequency, on a stratified mid-latitude continental
68 shelf (Lazure *et al.*, 2018). The extremely unstable physical nature of this sub-tidal
69 environment associated with the presence of poikilothermic organisms represents a true
70 ecological paradox, making this site a relevant place to study benthic organism responses to
71 chronic thermal variations.

72 Biogenic carbonate with recognizable periodic growth bands, such as bivalve molluscs can
73 incorporate minor and trace elements into their shells, in amounts depending on their
74 concentrations in the environment and on the physical and biological properties of the
75 surrounding seawater. However, bivalve shell biomineralization is a complex process, subject
76 to strong physiological and kinetic effects related to metabolism, growth rates, ontogenetic
77 age, shell mineralogy, crystal fabrics and organic matrix (e.g. Carré *et al.*, 2006; Freitas *et al.*,
78 2008; Freitas *et al.*, 2009; Freitas *et al.*, 2016; Klein *et al.*, 1996; Lazareth *et al.*, 2013; Lorens
79 and Bender, 1977; Schöne *et al.*, 2013; Shirai *et al.*, 2014). Owing to their wide geographic
80 distribution, economic importance, rapid growth rates, and the presence of annual growth
81 lines on their shell, pectinid bivalves (aka. scallops) offer good opportunities to document
82 past environmental conditions (Chauvaud *et al.*, 1998). The occurrence of a clearly visible
83 annual banding pattern on the upper valve of the Atlantic sea scallop, *Placopecten*
84 *magellanicus*, and the presence of this species in SPM over a wide bathymetric gradient (5 to
85 80 m), make this species a good candidate to track high-frequency past environmental
86 changes - reflected as variations in the shell geochemical properties – at extremely high
87 temporal resolution.

88 Spatially-resolved geochemical analysis of biogenic carbonates deposited between two
89 accurately dated growth lines can be performed with a wide set of methods, such as laser

90 ablation inductively coupled mass spectrometry (LA-ICPMS), secondary ion mass
91 spectrometry (nanoSIMS) or electron micro probe analyser (EMPA). Because of its potential
92 for rapid and accurate high-resolution *in situ* trace element analysis at relatively low cost and
93 minimal sample preparation requirements, LA-ICPMS has become a routine analytical tool in
94 a wide area of research applications (Warter and Müller, 2017).

95 As bivalve growth rates have often been related to environmental variables such as food
96 availability or water temperature (Ballesta-Artero *et al.*, 2017; Butler *et al.*, 2010; Marali and
97 Schöne, 2015; Witbaard *et al.*, 1997) and because of the importance of these two
98 parameters to track environmental and ecological changes, we then understand the interest
99 to track and calibrate elemental proxy records of these two variables. For example, some
100 authors proposed that magnesium to calcium ratios (Mg/Ca) can be used to record water
101 temperature (Ullmann *et al.*, 2013, Bougeois *et al.*, 2014), while there are many reports of
102 strong vital effects in bivalve shells for this element (Lorrain *et al.*, 2005, Wanamaker *et al.*,
103 2008, Surge and Lohmann, 2008). Uranium-to-calcium ratio has also been suggested as a
104 proxy for temperature in shallow-water corals (Min *et al.*, 1995; Shen and Dunbar, 1995) and
105 in planktonic foraminiferal carbonates (Yu *et al.*, 2008). Some authors also found a pH effect
106 on U/Ca ratios in both inorganic aragonite and calcite (Kitano and Oomori, 1971; Chung and
107 Swart, 1990). Indeed, U/Ca ratios in calcium carbonate are negatively correlated with pH and
108 $[\text{CO}_3^{2-}]$, because in aqueous solutions the carbonate ion complexes with the uranyl ion
109 (UO_2^{2+}) at higher pH (Langmuir, 1978), therefore less uranium is available to be incorporated
110 in shell carbonate. Regarding U/Ca ratio on mollusc shells, Frieder *et al.* (2014)
111 demonstrated that U/Ca varies as a function of pH in shells of living larvae in *Mytilus*
112 *californianus* and *Mytilus galloprovincialis*. More recently, Zhao *et al.* (2018) demonstrated
113 by measuring U/Ca ratio on *Mya arenaria* shells exposed to $p\text{CO}_2$ -enriched environments the
114 existence of efficient regulatory mechanisms to tightly control the pH at the site of
115 calcification of this species. . Ba/Ca profiles in bivalve shells are typically characterized by a
116 flat background signal interrupted by sharp peaks. Background level has been suggested to
117 be linked with salinity (Gillikin *et al.*, 2006, 2008). As for peaks, many authors suggested a
118 synchronization with phytoplankton blooms (e.g. Elliot *et al.*, 2009; Lazareth *et al.*, 2003;
119 Stecher *et al.*, 1996; Thébault *et al.*, 2009; Vander Putten *et al.*, 2000). Building on the work
120 of Stecher and Kogut (1999), Thébault *et al.* (2009) proposed two main hypotheses to

121 explain the peaks: (1) ingestion of barite originating from assemblages of recently dead
122 diatoms or (2) adsorption of barium onto iron oxyhydroxides associated with diatoms
123 frustules.

124 The main objective of our study was to identify whether the calcitic shell of *P. magellanicus*
125 can record the high frequency (25.8 h) environmental variations observed in SPM. To this
126 end, we have developed a new ultra-high resolution LA-ICPMS analytical method in order to
127 investigate skeletal trace element concentration with a 10 μm resolution. Results of our
128 investigation can contribute to a better understanding of environmental and physiological
129 mechanisms associated to sub daily environmental variations on ions incorporation into fast
130 growing marine bivalve shells.

131 **2. Materials and Methods**

132 **2.1 Sample collection**

133 Two live *P. magellanicus* were collected in September 2016 from Saint-Pierre Bay (Saint-Pierre
134 and Miquelon – NW Atlantic) respectively at 10 m and 30 m depth (Figure 1). Both individuals
135 were in their fourth year of growth. The deepest location consisted in a homogeneous
136 substrate, made of compacted and stable fine sand. At the shallowest one, the substrate was
137 more heterogeneous and consisted of a mixture of gravels, pebbles, and rocks with a
138 seaweed cover. Soft tissues were removed immediately after collection. Both shells were
139 carefully cleaned with freshwater to remove adherent sediment and biological tissues before
140 sample preparation.



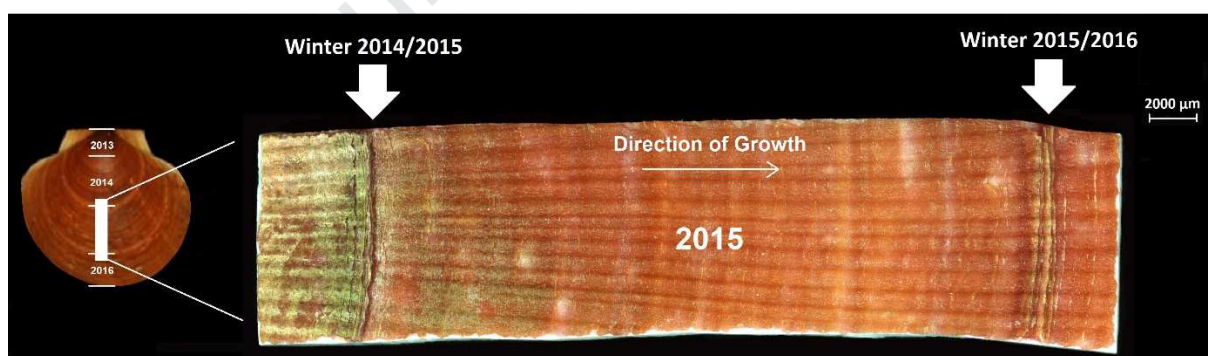
142 **Figure 1:** (A) Location of Saint-Pierre and Miquelon archipelago. (B) Satellite image of *P.*
 143 *magellanicus* sampling sites (red dots) in Saint-Pierre Bay.

144 2.2 Environmental monitoring

145 Annual thermal profiles at 10 m and 30 m discussed were derived from Lazure *et al.* (2018)
 146 study. To refine our vision of thermal variations on the two collection sites (Figure 1), three
 147 multi-parameter probes measuring temperature every 5 minutes were deployed at 8 m, 12
 148 m and 30 m depth, between 28/08/2017 and 15/09/2017. The 2015 monthly satellite
 149 chlorophyll *a* measurements were downloaded from the GlobColour website
 150 (<http://hermes.acri.fr>) and are weighted monthly averages of single-sensor products
 151 (SeaWiFS/MERIS/MODIS/VIIRS merged chlorophyll concentrations) over the area 46.6–
 152 47.3°N / 56.0–56.6°W (i.e., waters surrounding the SPM archipelago within ca. 30 km).

153 2.3 Sample preparation

154 All micro-chemical analyses were performed on *P. magellanicus* upper valves. Indeed, the
 155 lower valves might have been contaminated as a result of a prolonged contact with the
 156 sediment. For each individual, a fragment of shell of ca. 3.5 cm x 1 cm was cut with a
 157 diamond saw, including the axis of maximal growth (Figure 2).



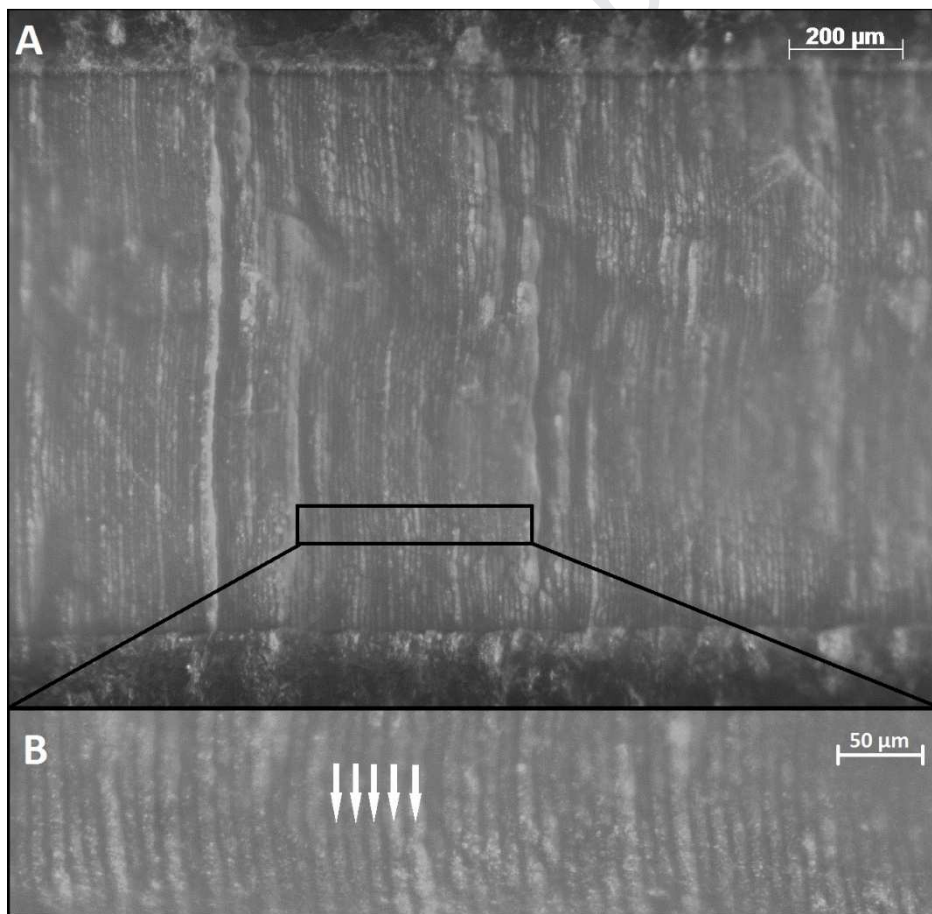
158
 159 **Figure 2:** Example of one *P. magellanicus* fragment used for LA-ICPMS analyses. White
 160 arrows indicate annual shell growth lines positions defining 2015 increment.

161 All ultra-high resolution LA-ICPMS analyses were performed on these two shell portions.
 162 These fragments represent, for each individual, the third year of growth corresponding to
 163 2015 annual growth periods. The outer shell layer was ultrasonically cleaned with deionized
 164 water to remove organic matter and sediment particles. In addition, before LA-ICPMS

165 analyses, the outer shell layer of each sample was chemically cleaned with a 15 seconds
166 acetic acid (10 %) bath, soaked in deionized water during 10 seconds, and left to air dry in
167 the LA-ICPMS clean room.

168 2.4 Ultra-high resolution fs-LA-ICPMS analysis

169 A UV high-repetition-rate femtosecond laser ablation (fs-LA) system (Nexeya SA, Canejan,
170 France) was employed (Pulse duration: 360fs; wavelength: 257 nm). Each ICPMS
171 measurement point represents an ablation transect with a 1-mm long arcuate trajectory,
172 parallel to the ventral margin, made by fast round trips of a 10 μm spot (Figure 3). All
173 transects were adjacent in order to analyse the whole “2015 annual period of growth” for
174 the two individuals. The area, covered by a 1 mm x 10 μm transect is equivalent to the area
175 covered by a 110 μm diameter round spot.



176

177 **Figure 3:** Post ablation picture of a 1.5 mm *P. magellanicus* section showing ca. 150
178 femtosecond laser ablation transects (A). Zoom on a small fraction of them, each white

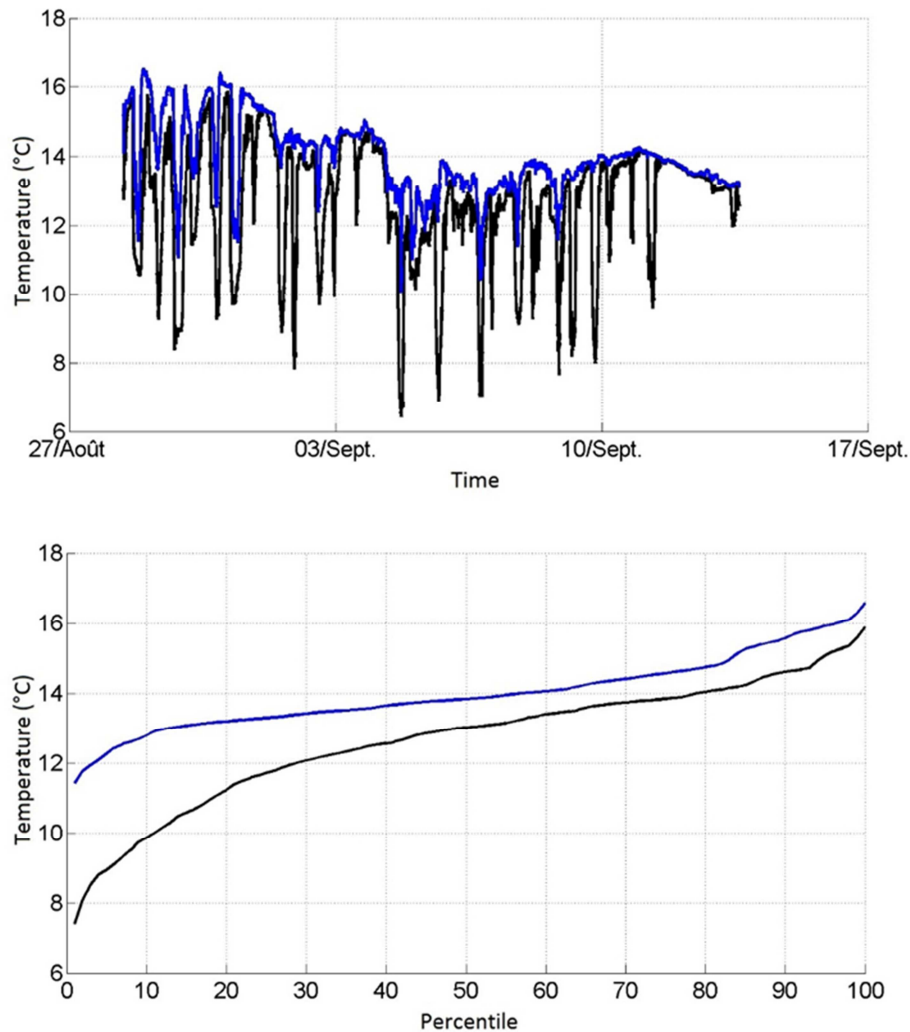
179 arrow points to a laser ablation transect (B). The visible lines represent ridges generated
180 during the laser ablation process.

181 Outer shell layers were analysed for Mg/Ca, Ba/Ca and U/Ca ratios using a high-resolution
182 inductively coupled plasma mass spectrometer fitted with a jet interface (Element XR,
183 Thermo Scientific, USA). A helium gas stream carried ablated material to the HR-ICP-MS
184 (carrier gas flow rate 0.68 L.min⁻¹). Elemental ratios were quantified by monitoring ⁴³Ca,
185 ²⁴Mg, ¹³⁸Ba, and ²³⁸U. Calcium was used as an internal standard. Elements were standardized
186 to calcium based on the stoichiometry of calcium carbonate (388 000 µgCa.g⁻¹ outer shell
187 layer), assuming 100 % CaCO₃: Mg/Ca (µg.g⁻¹), Ba/Ca (µg.g⁻¹) and U/Ca (µg.g⁻¹).
188 Quantification of trace elements in otoliths was achieved by external calibration using both
189 carbonate pellets FEBS-1 (Barats et al., 2007) and 2 NIST glass standards (610, 612) to ensure
190 the best accuracy. Each standard was analysed three times before and after each session
191 with the laser to account for drifting during the day. The limits of detection (µg.g⁻¹ in shells)
192 achieved in this study were 0.08, 0.01 and 0.002 for ²⁴Mg, ¹³⁸Ba, and ²³⁸U, respectively.
193 They were based on a 3σ criterion, where σ is the standard deviation of the mean blank
194 count for each isotope. All the elemental concentrations in the outer shell layer were above
195 the detection limits.

196 **3. Results**

197 **3.1 Environmental parameters:**

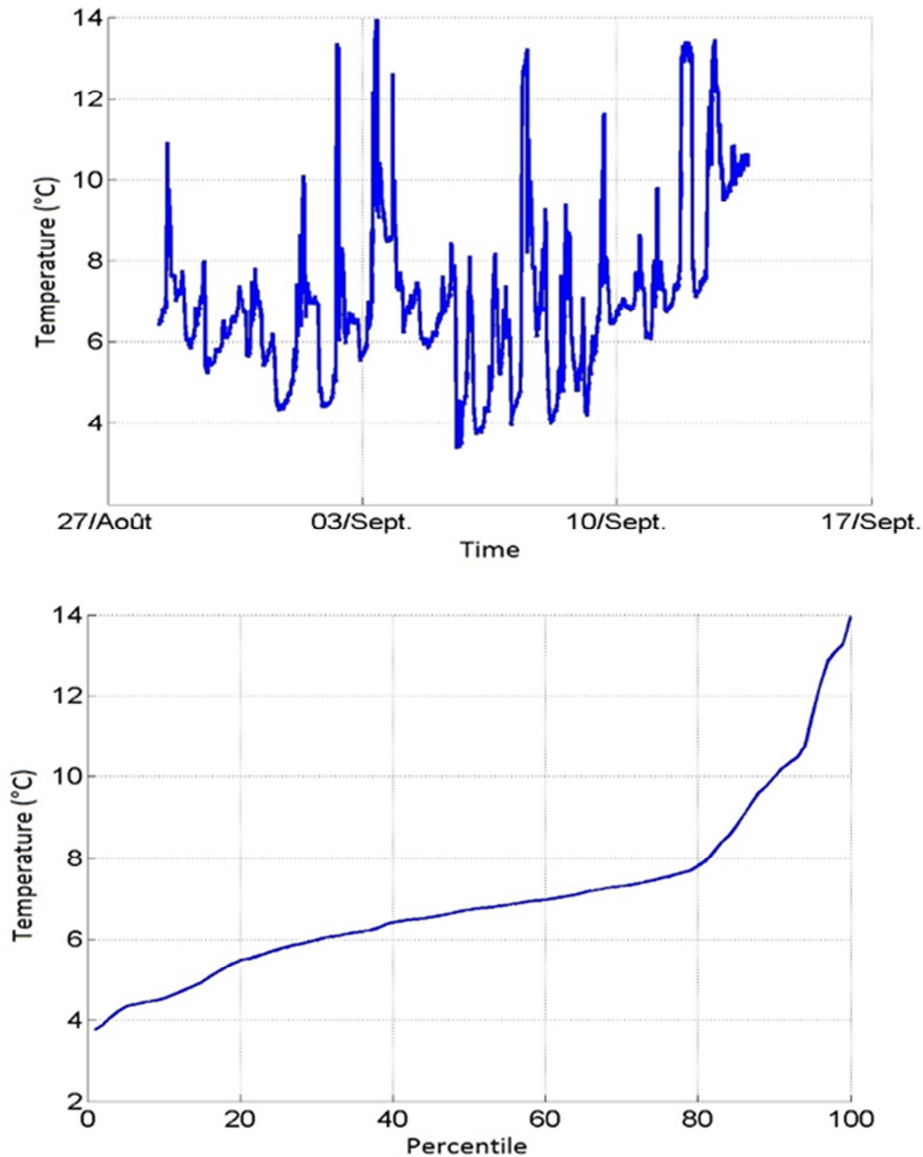
198 Around 10 m depth, the temperature varied from 2 °C in May to a maximum of 16 °C in early
199 September and then decreased to 8 °C in November. At this depth, seawater temperature
200 presents a classic seasonal cycle with cold water intrusions (Figure 4). During the first two
201 weeks of September at 8 m and 12 m in Saint-Pierre Bay, temperature showed high-
202 frequency variations with cold water incursions leading to 4°C (8m) to 6°C (12m) amplitudes
203 (Figure 4). Along these two weeks, temperatures were 70% of the time above 12 °C (Figure
204 4).



205

206 **Figure 4:** End of August and first two weeks of September 2017 time series of seawater
 207 temperatures at 8 m and 12m depth (blue and black) (top graphic). Percentile distribution of
 208 these temperatures at 8 m and 12m depth (blue and black).

209 At 30 m depth, the temperature annual profile was radically different (Figure 5). Seawater
 210 temperature baseline is mainly cold over the year, showing low seasonal amplitudes.
 211 However, during the stratified period, temperatures showed high-frequency variations
 212 whose amplitude increased with sea-surface temperature. During the first two weeks of
 213 September (Figure 5), oscillations were the largest in term of amplitude, reaching nearly
 214 10°C. Along these two weeks, temperatures were 80% of the time below 8 °C (Figure 5).

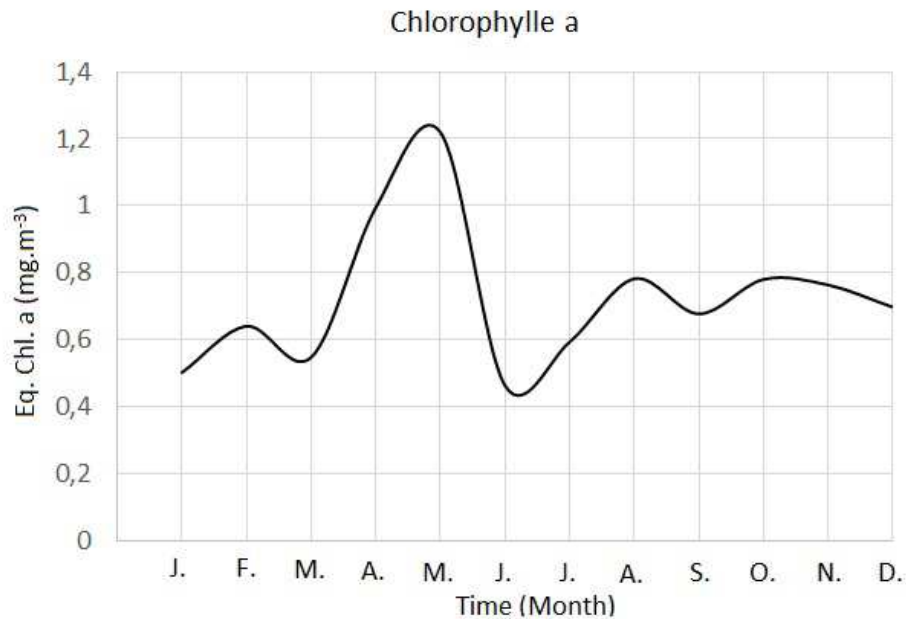


215

216 **Figure 5:** End of August and first two weeks of September 2017 time series of seawater
217 temperatures at 30m depth (top graphic). Percentile distribution of these temperatures
218 during these two weeks.

219

220 Monthly mean satellite chlorophyll *a* concentrations ranged from 0.46 to 1.22 mg.m⁻³ (Figure
221 6). The annual time series-exhibited a background level around 0.7 mg.m⁻³, with one major
222 peak in April - May 2015.



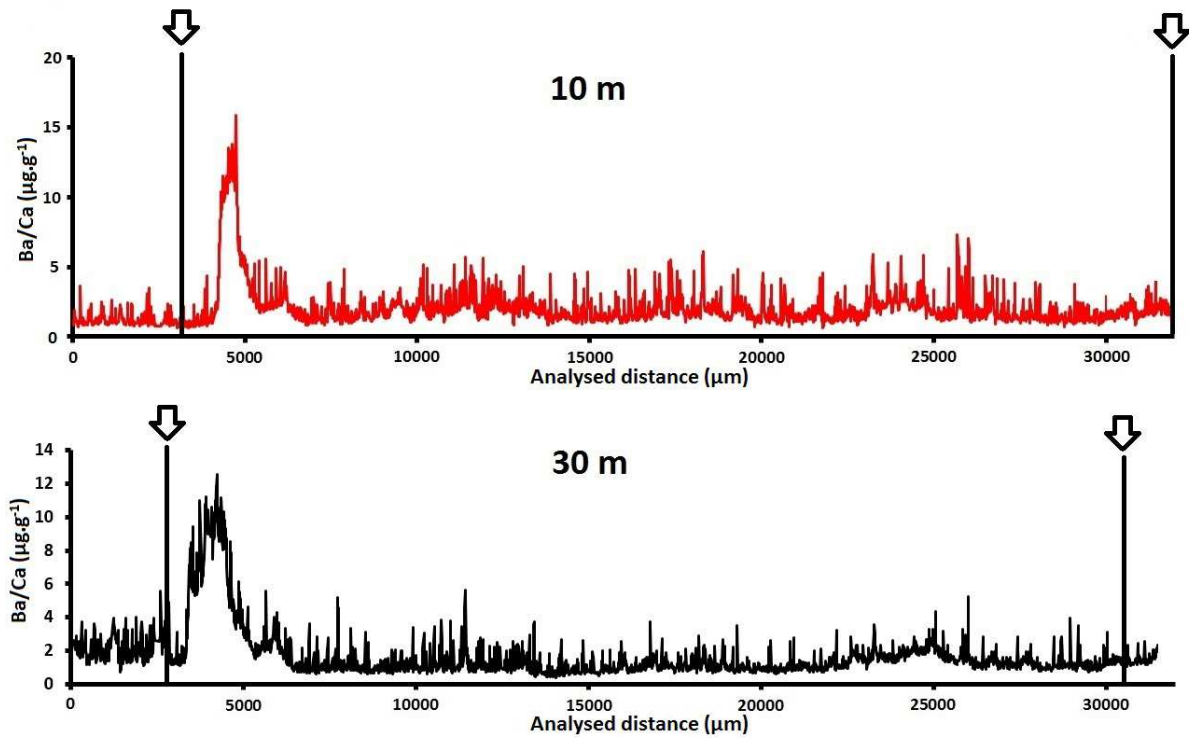
223

224 **Figure 6:** Monthly satellite equivalent chlorophyll a (mg.m⁻³) measurements over the year
 225 2015.

226

227 3.2 Ba/Ca ratio profiles in the shell carbonates

228 Outer shell layer Ba/Ca ratios ranged from 0.61 to 15.71 $\mu\text{g.g}^{-1}$ at 10 m and from 0.43 to
 229 12.54 $\mu\text{g.g}^{-1}$ at 30 m (Figure 7). Both series have the same profile with one major peak
 230 occurring respectively 370 μm and 830 μm after the “winter 2014/2015” growth line. The
 231 main Ba/Ca peak covers 1370 and 2220 μm of shell at 10 and 30 m, respectively. A
 232 secondary smaller Ba/Ca peak occurred immediately after the first one, covering respectively
 233 1230 and 1160 μm at 10 and 30 m. Ba/Ca baseline was the same for the two time-series
 234 (around 1.5 $\mu\text{g.g}^{-1}$).



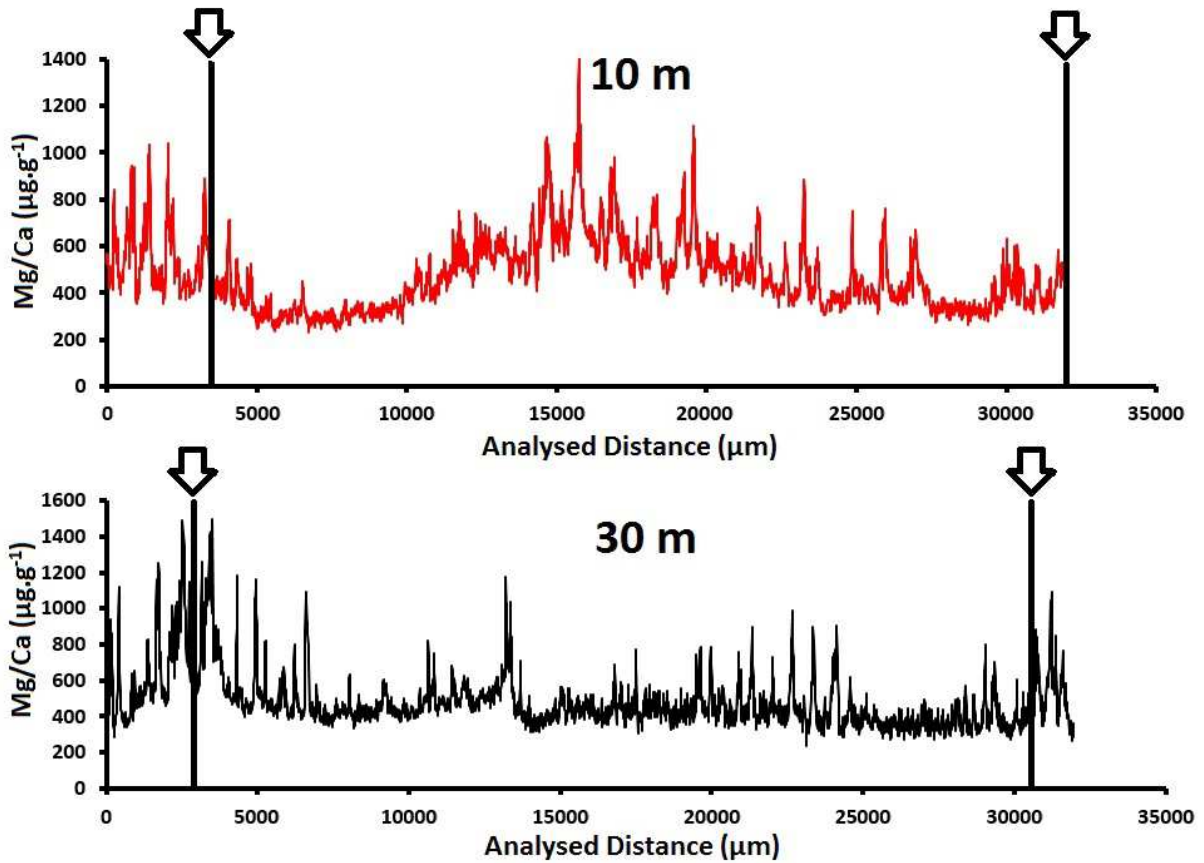
235

236 **Figure 7:** Ba/Ca ($\mu\text{g}\cdot\text{g}^{-1}$) series at 10 m (red curve) and 30 m (black curve). Vertical lines
 237 placed under the arrows indicate the position of winter shell growth lines.

238

239 3.3 Mg/Ca ratio profiles

240 Outer shell layer Mg/Ca ratios ranged from 232 to 1408 $\mu\text{g}\cdot\text{g}^{-1}$ at 10 m and from 233 to 1495
 241 $\mu\text{g}\cdot\text{g}^{-1}$ at 30 m (Figure 8). At 10 m, Mg/Ca profile followed a sinusoidal pattern with stronger
 242 high frequency variations between 15 000 and 25 000 μm (top and decreasing phase, Figure
 243 8). At 30 m depth, the Mg/Ca profile was radically different with a globally flat profile
 244 between the two growth lines and high frequency variations mainly between 15000 and
 245 25000 μm (Figure 8).



246

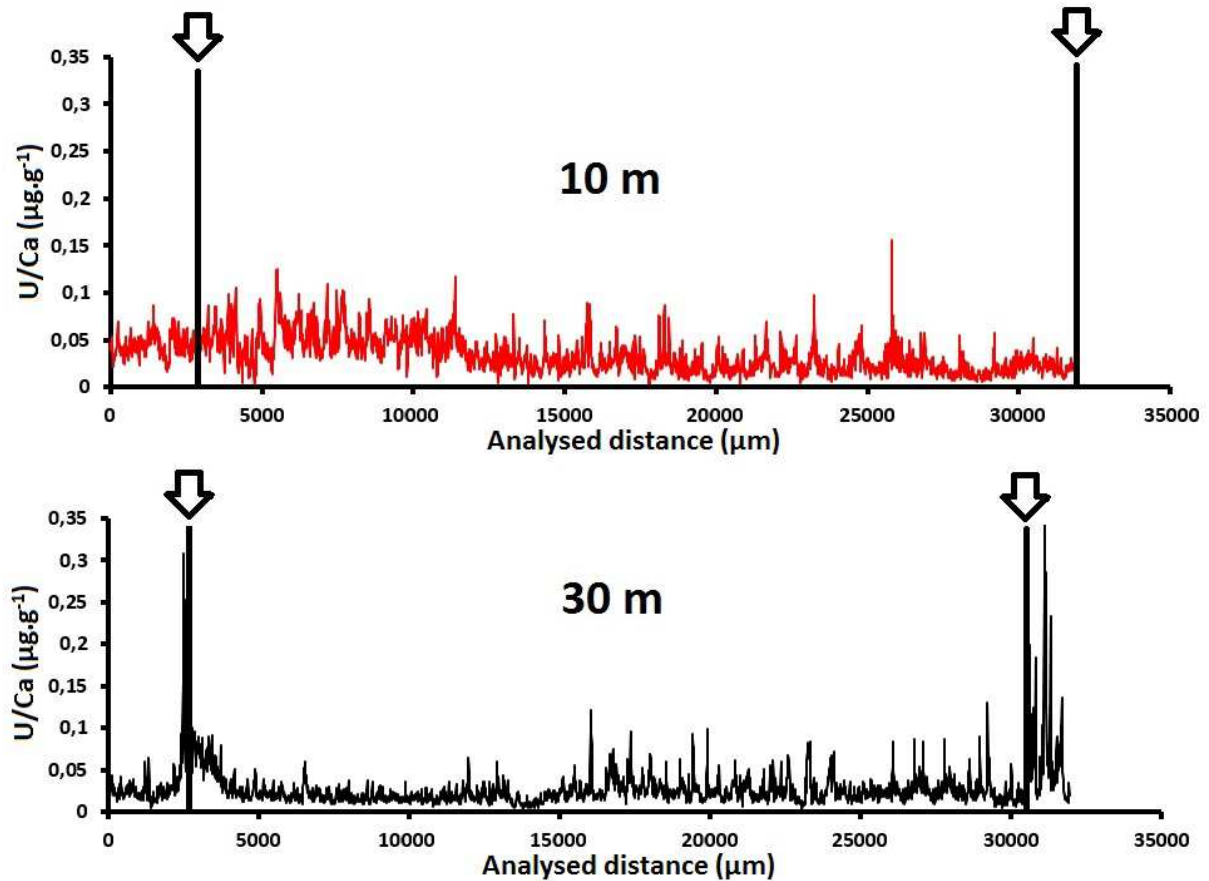
247 **Figure 8 :** Mg/Ca ($\mu\text{g}\cdot\text{g}^{-1}$) series at 10 m (red curve) and 30 m (black curve). Vertical lines
 248 placed under the arrows indicate the position of shell growth lines.

249

250

3.4 U/Ca ratio profiles

251 Outer shell layer U/Ca ratios ranged from 0.003 to 0.16 $\mu\text{g}\cdot\text{g}^{-1}$ at 10 m and from 0.004 to 0.36
 252 $\mu\text{g}\cdot\text{g}^{-1}$ at 30 m (Figure 9). At 10 m depth, U/Ca time series had a relatively flat pattern with high-
 253 frequency variations all along the profile. At 30 m depth, U/Ca profile was close to Mg/Ca one.
 254 So we decided to compare those profiles in the next paragraph.



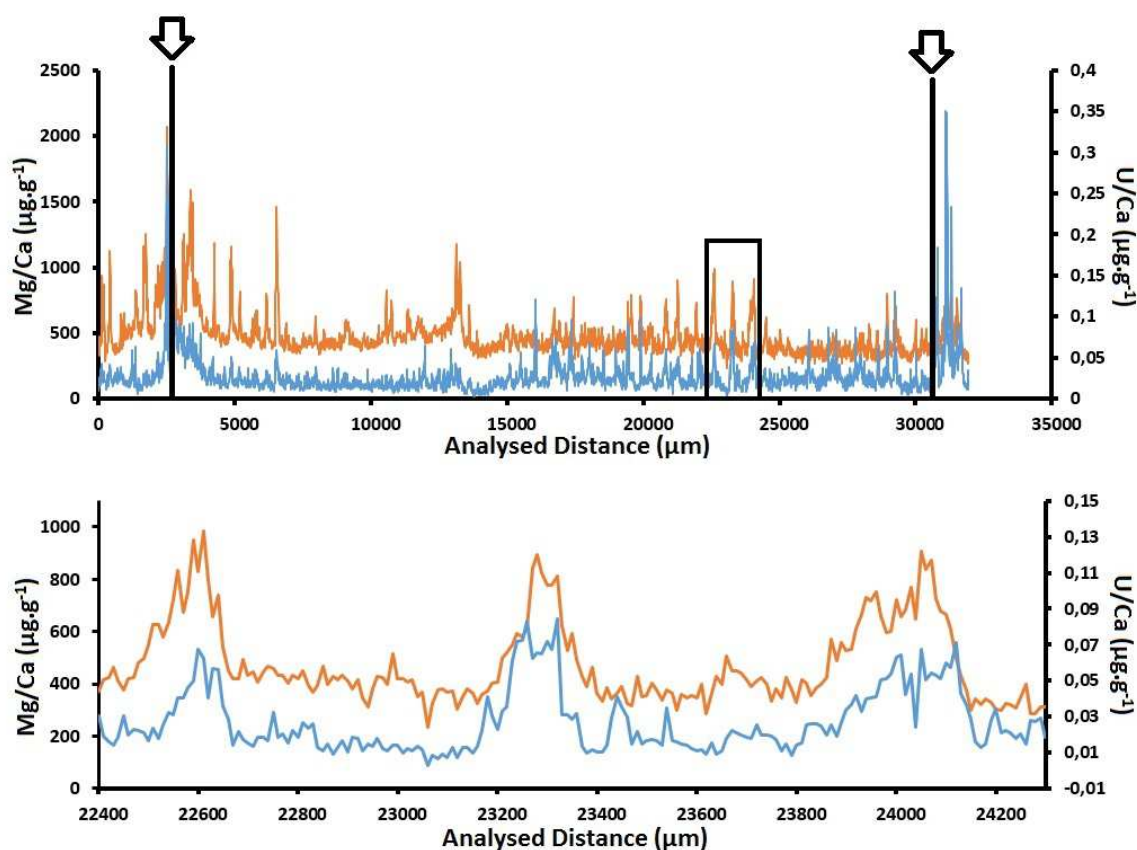
255

256 **Figure 9:** U/Ca ($\mu\text{g}\cdot\text{g}^{-1}$) series at 10 m (red curve) and 30 m (black curve). Vertical lines placed
 257 under the arrows indicate the position of shell growth lines.

258

259 3.5 U/Ca and Mg/Ca comparison at 30m depth:

260 At 30 m depth, U/Ca and Mg/Ca profiles presented a strong positive correlation ($N = 3135$, r
 261 $= 0.62$, $p < 0.001$) (Figure 10). A closer examination of this relationship on a shorter time
 262 window (i.e. three high frequency cycles, between 22400 μm and 24250 μm) revealed an
 263 even stronger correlation ($N = 186$, $r = 0.77$, $p < 0.001$).



264

265 **Figure 10:** U/Ca ($\mu\text{g}\cdot\text{g}^{-1}$) (blue curve) and Mg/Ca ($\mu\text{g}\cdot\text{g}^{-1}$) (orange curve) series at 30 m.
 266 Vertical lines placed under the arrows indicate the position of shell growth lines. The graph
 267 below represents a close-up on three peaks (black box in the upper graph).

268 **4. Discussion**

269

270 This paper presents the first chemical analyses performed on *P. magellanicus* shells.
 271 Regarding the temporal resolution (25.82 h) of the environmental phenomena we wanted to
 272 track, it was necessary to develop a new analytical method. Our novel approach using ultra-
 273 high resolution fs-LA-ICPMS enables trace element analyses in bivalve shells with a 10- μm
 274 resolution. This study gave us first insights about *P. magellanicus* ability to record high-
 275 frequency environmental variations within its shell.

276 **4.1 Barium**

277 The high degree of similarity between the two Ba/Ca profiles suggests that the occurrence of
 278 Ba/Ca peaks was controlled by one or multiple common environmental factors. The pattern

279 of these two Ba/Ca profiles is similar to those observed in cross sections of other bivalve
280 species (e.g., Gillikin *et al.*, 2008; Stecher *et al.* 1996; Vander Putten *et al.*, 2000). This
281 confirms the hypothesis which suggests that the choice of analyzing the shell surface or the
282 outer shell layer in cross sections do not have significant influence on Ba/Ca records in shells.
283 In this section, we will discuss several hypotheses to explain temporal variability of Ba/Ca in
284 *P. magellanicus* shell. Background levels of Ba/Ca time-series in bivalve shells have been
285 suggested to record salinity variations (e.g. Gillikin *et al.*, 2006). There is generally a linear
286 inverse relationship between seawater salinity and dissolved barium concentrations (Coffey
287 *et al.*, 1997; Gillikin *et al.*, 2006). However, variability in seawater dissolved barium
288 concentrations as a source for the Ba/Ca peaks in *P. magellanicus* from SPM is highly
289 unlikely. Indeed, SPM islands, due to their offshore status, are not subjected to major
290 riverine inputs and associated variations in salinity (Poitevin *et al.*, 2018). Salinity usually
291 ranges from 31.3 to 32.2 PSU (see Figure 4 in Poitevin *et al.*, 2018) without a clear seasonal
292 trend and, therefore, cannot explain Ba/Ca peaks measured in the shells. Many authors
293 suggested a close relationship between these Ba/Ca peaks and phytoplankton blooms (e.g.
294 Elliot *et al.*, 2009; Lazareth *et al.*, 2003; Stecher *et al.*, 1996; Thébault *et al.*, 2009; Vander
295 Putten *et al.*, 2000). In our study, the high similarity of chlorophyll *a* concentration (Figure 6)
296 and Ba/Ca (Figure 7) profiles strongly suggest a relationship between phytoplankton biomass
297 and barium incorporation into *P. magellanicus* shells. Indeed, the occurrence of this bloom,
298 in May 2015, seems to be consistent with the starting of *P. magellanicus* annual growth from
299 other Canadian regions (Chute *et al.* 2012; Kleinman *et al.*, 1996). Elevated levels of
300 suspended barite (BaSO₄) have been suggested to be linked with oceanic diatoms primary
301 productivity (Dehairs *et al.*, 1991). Most of the barium released by diatoms after a bloom is
302 labile and only a minor fraction eventually forms barite crystals (Ganeshram *et al.*, 2003).
303 Therefore, if labile barium, either in phytoplankton or released into the dissolved phase, was
304 the cause of the Ba/Ca peaks, these peaks should form near the end of the bloom or very
305 shortly thereafter (Gillikin *et al.*, 2008). Considering the absence of daily growth lines in *P.*
306 *magellanicus*, we cannot conclude about chlorophyll *a* and Ba/Ca peaks timing. Finally, the
307 two Ba/Ca profiles exhibited a double peak, with a first large amplitude one and a smaller
308 second peak. This observation has also been made in *P. maximus* Ba/Ca profiles (Gillikin *et*
309 *al.*, 2008). One explanation for this double peak proposed in this study is based on
310 Ganeshram *et al.* (2003). They found that barite formation can take several weeks to reach

311 its maximum after the beginning of phytoplankton decay. Barite may be formed at the
312 sediment surface and be ingested by *P. magellanicus* several weeks after the phytoplankton
313 bloom ends.

314 These observations on Ba/Ca incorporation in *P. magellanicus* shell from SPM imply a real
315 need for complementary information related to local *P. magellanicus* growth dynamics and
316 physiology. It would also be crucial to get insights about the nature and the quantity of
317 benthic and pelagic primary production over the year and along a bathymetric gradient.

318

319 **4.2 Magnesium**

320 In bivalve shells, the relationship between seawater temperature and Mg/Ca ratio is still
321 subject to controversy. Some authors proposed that Mg/Ca ratios can be used to record
322 water temperature (e.g., Bougeois *et al.*, 2014; Lazareth *et al.*, 2003; Mouchi *et al.*, 2013;
323 Surge and Lohmann, 2008; Ullmann *et al.*, 2013), while there are many reports of strong vital
324 effects in bivalve shells for this element (e.g., Elliot *et al.*, 2009; Lorrain *et al.*, 2005,
325 Wanamaker *et al.*, 2008). In this study, we can hardly discuss the importance of vital effects
326 on trace elements incorporation into *P. magellanicus* shell. Indeed, our analyses were only
327 carried out on one year of growth (ontogenetic and calendar) and one individual per site.
328 The only thing we can say about physiological control of Mg incorporation in *P. magellanicus*
329 shell is based on Mg/Ca level. In this study, the mean Mg/Ca ratio ($\sim 500 \mu\text{g.g}^{-1}$ corresponding
330 to $\sim 2 \text{mmol.mol}^{-1}$) of the calcitic outer shell layer of *P. magellanicus* corresponds to a low
331 value compared to other calcitic mollusc shells (Lazareth *et al.*, 2007 and references therein).
332 Given the absence of sclerochemical studies about trace element incorporation in *P.*
333 *magellanicus* shells, we can only try to explain these low Mg concentrations relying on
334 studies based on other calcitic bivalves with low Mg/Ca concentrations. For example, Lorens
335 and Bender (1977) suggested that *Mytilus edulis* biologically regulates the amount of Mg
336 entering the extrapallial fluid to produce low-Mg calcite. Perhaps a similar process occurs in
337 *P. magellanicus*, suggesting a physiological control of Mg incorporation that could obscure
338 Mg/Ca and seawater temperature relationship. This confirms the need for additional
339 investigations on biomineralization, e.g. through experiments in controlled environments, in
340 order to better understand trace elements incorporation in *P. magellanicus* shell. However,

341 the shape of the two Mg/Ca profiles tend to highlight kind of a temperature control on
342 magnesium incorporation in our shells. At 10 m, the sinusoidal pattern of Mg/Ca ratio may
343 reflect the seasonal seawater temperature annual cycle at 10 m depth. While at 30 m, the
344 Mg/Ca profile presents a relatively flat baseline with high-frequency variations, which could
345 mirror the seawater seasonal temperature trend, namely showing low seasonal amplitudes
346 with high-frequency variations (Lazure *et al.*, 2018). Other studies also point to the non-
347 systematic relationship between Mg/Ca ratio and SST. From a one year study of *M. edulis*
348 growth, Vander Putten *et al.* (2000) observed a positive correlation between Mg/Ca and SST
349 only during spring. Small-scale variations in Mg concentrations in *M. edulis* calcite have also
350 been shown to derive from Mg being concentrated along the margins of calcite prisms
351 (Rosenberg *et al.*, 2001). Indeed, the absence of interannual growth lines on the *P.*
352 *magellanicus* shell is problematic to convert analysed distances in time. That is why enhance
353 our knowledge on *P. magellanicus* growth dynamics along this bathymetric gradient in SPM
354 would help us decipher physiological and environmental effects on trace element
355 incorporation in *P. magellanicus* shell calcite. In addition, the lack of high frequency
356 environmental data limits our ability to fully interpret our results and confirms the interest
357 to set up a high frequency observatory along this bathymetric gradient.

358

359 4.3 Uranium

360 In our study, U/Ca and Mg/Ca profiles show a strong positive correlation in shells collected
361 at 30 m (N=3135, $r=0.62$, $p<0.001$) (Fig. 10). However, this is not the case for the shallowest
362 shells for which no significant correlation could be found. These results suggest that (i)
363 environmental uranium availability for *P. magellanicus* are not the same between the two
364 sites and/or (ii) that physiological differences between *P. magellanicus* from 10 m and 30 m
365 sites could lead to differential incorporation of uranium in shells.

366 Since (i) we do not have information about *P. magellanicus* physiological differences
367 between these two depths, and (ii) only few studies previously investigated U/Ca ratio as a
368 potential paleo environmental proxy in bivalve shells (Frieder *et al.*, 2014; Gillikin and
369 Dehairs, 2012; Zhao *et al.*, 2018), it seems difficult to draw conclusions about the kind of
370 processes influencing uranium incorporation in *P. magellanicus* shells.

371 To our knowledge, U/Ca ratio as a paleo environmental proxy has been studied for the first
372 time in mollusc shell by Gillikin and Dehairs (2012). In this study the authors tried to
373 investigate U/Ca in *Saxidomus gigantea* shell as a potential acidification proxy and concluded
374 that U/Ca may not reflect environmental variability and did not function as a paleo-pH proxy.
375 More recently, Zhao *et al.* (2018) also found virtually unchanged U/Ca values in *Mya*
376 *arenaria* shells with increasing seawater $p\text{CO}_2$ up to 2900 μatm . However, in the same study
377 the authors found a significant increase in U/Ca ratio in shells with the increase in seawater
378 $p\text{CO}_2$ at 6600 μatm . These findings reveal the existence of certain compensatory mechanisms
379 by which this species may partially mitigate the impact of high environmental $p\text{CO}_2$ on shell
380 formation through modifying the calcifying fluid chemistry to maintain its pH homeostasis
381 (Zhao *et al.*, 2018). These conclusions lead us to consider *P. magellanicus* physiological
382 responses induced by the repeated thermal variations occurring at the 31m site and their
383 impact on the calcifying fluid pH of this species. Considering our study purpose and
384 resolution, it seems difficult to conclude about U/Ca as a potential acidification proxy in *P.*
385 *magellanicus* shell, especially as we do not have pH measurements on our study sites.
386 Uranium-to-calcium ratios have also been suggested as a proxy for temperature in shallow
387 water corals (e.g., Min *et al.*, 1995; Shen and Dunbar, 1995) and in planktonic foraminiferal
388 carbonates (e.g., Yu *et al.*, 2008). In our study, the positive correlation between U/Ca and
389 Mg/Ca profiles in the shell collected at 30 m would support this hypothesis. However, this
390 correlation does not hold anymore at 10 m, suggesting that variations in uranium
391 bioavailability differs between our two sites. Indeed, microorganisms have the ability to
392 adsorb radionuclides/metals through extracellular binding involving physical adsorption, ion
393 exchange, complexation and precipitation (Acharya *et al.*, 2009). They also sequester the
394 metal ions by passive/active transport to the interior of the cell, followed by its
395 accumulation. Microbial cells have been shown to reduce, oxidize, adsorb, accumulate and
396 precipitate uranium (Fredrickson *et al.*, 1999; Macaskie *et al.*, 2000). So differences in
397 microbial communities between the two sites, related to the nature of the habitat or to
398 depth, could lead to changes in environmental uranium availability and finally to shell U/Ca
399 ratios.

400 **5. Conclusion**

401 Our novel approach using ultra-high resolution fs-LA-ICPMS enables trace element analyses
402 in bivalve shells with a 10- μm resolution. This study gave us first insights about *P.*
403 *magellanicus* ability to record high-frequency environmental variations within its shell at a
404 sub-hourly scale.

405 From an analytical point of view, it would be interesting to continue this study by applying
406 this new analytical technique to more individuals. This would allow us to discuss about inter-
407 individual variability within those two sites. Moreover, combining this approach with nano-
408 SIMS $\delta^{18}\text{O}$ measurements (temperature proxy) would help us to get insights about the
409 temperature control of Mg and U incorporation in shells.

410 In terms of data interpretation, these results also confirm a real need for complementary
411 information. Some of them should be related to *P. magellanicus* intra-annual growth
412 dynamics. Indeed, in this study the absence of visible intra-annual growth lines visible on *P.*
413 *magellanicus* shells hindered the temporal alignment of our microchemical data. Others
414 must concern *P. magellanicus* physiological responses and their impacts on the calcifying
415 fluid chemistry of this species. All these additional studies will require multiple high
416 frequency environmental data continuously recorded at an individual scale within those two
417 sites.

418 **6. Acknowledgements**

419 First, we thank the LEMAR (UMR 6539) Secretariat team (Anne-Sophie Podeur, Geneviève Cohat, and
420 Yves Larsonneur) for their invaluable assistance during the administrative preparation of the
421 analytical trip associated with this work in Pau. We also thank Gaëlle Barbotin for her help during fs-
422 LA-ICPMS measurements in Pau. This work was supported by the EC2CO program MATISSE of the
423 CNRS INSU, the Cluster of Excellence LabexMER, and the LIA BeBEST CNRS INEE. This research was
424 carried out as part of the Ph.D. thesis of Pierre Poitevin for the University of Western Brittany with a
425 French Ministry of Higher Education and Research grant. This manuscript greatly benefited from very
426 useful comments made by the reviewers.

427 **7. References**

428 Acharya C, Joseph D, Apte SK (2009) Uranium sequestration by a marine cyanobacterium
429 *Synechococcus elongatus* strain BDU/75042. *Bioresource Technology*, **100**, 2176-2181.

- 430 Ballesta-Artero I, Witbaard R, Carroll ML, Van der Meer J (2017) Environmental factors
431 regulating gaping activity of the bivalve *Arctica islandica* in Northern Norway. *Marine*
432 *Biology*, **164 (5)**, 116.
- 433 Barats A, Amouroux D, Pecheyran C, Chauvaud L, Donard OFX (2007) High-Frequency
434 Archives of Manganese Inputs To Coastal Waters (Bay of Seine, France) Resolved by the LA
435 ICPMS Analysis of Calcitic Growth Layers along Scallop Shells (*Pecten maximus*).
436 *Environmental Science & Technology*, **42 (1)**, 86-92.
- 437 Bougeois L, de Rafélis M, Reichart GJ, de Nooijer LJ, Nicollin F, Dupont-Nivet G (2014) A high
438 resolution study of trace elements and stable isotopes in oyster shells to estimate Central
439 Asian Middle Eocene seasonality. *Chemical Geology*, **363**, 200-212.
- 440 Butler PG, Richardson CA, Scourse JD, et al. (2010) Marine climate in the Irish Sea: analysis of
441 a 489-year marine master chronology derived from growth increments in the shell of the
442 clam *Arctica islandica*. *Quaternary Science Reviews*, **29**, 1614–1632.
- 443 Carré M, Bentaleb I, Bruguier O, Ordinola E, Barrett NT, Fontugne M (2006) Calcification rate
444 influence on trace element concentrations in aragonitic bivalve shells: Evidences and
445 mechanisms. *Geochimica et Cosmochimica Acta*, **70**, 4906-4920.
- 446 Chauvaud L, Thouzeau G, Paulet YM (1998) Effects of environmental factors on the daily
447 growth rate, *Journal of Experimental Marine Biology and Ecology*, **227**, 83–111.
- 448 Chung GS, Swart PK (1990) The concentration of uranium in freshwater vadose and phreatic
449 cements in a Holocene ooid cay; a method of identifying ancient water tables. *Journal of*
450 *Sedimentary Research*, **60**, 735-746.
- 451 Chute AS, Wainright SC, Hart DR (2012) Timing of shell ring formation and patterns of shell
452 growth in the sea scallop *Placopecten magellanicus* based on stable oxygen isotopes. *Journal*
453 *of Shellfish Research*, **31**, 649- 662.
- 454 Coffey M, Dehairs F, Collette O, Luther G, Church T, Jickells T (1997) The behaviour of
455 dissolved barium in estuaries. *Estuarine, Coastal and Shelf Science*, **45**, 113-121.
- 456 Dehairs F, Stroobants N., Goeyens L (1991) Suspended barite as a tracer of biological activity
457 in the Southern Ocean. *Marine Chemistry*, **35**, 399–410.

- 458 Elliot M, Welsh K, Chilcott C, McCulloch M, Chappell J, Ayling B (2009) Profiles of trace
459 elements and stable isotopes derived from giant long-lived *Tridacna gigas* bivalves: Potential
460 applications in paleoclimate studies. *Palaeogeography, Palaeoclimatology, Palaeoecology*,
461 **280**, 132-142.
- 462 Fredrickson JK, Kostandarithes HM, Li SW, Plymale AE, Daly MJ (1999) Reduction of Fe(III),
463 Cr(VI), U(VI) and Te(VII) by *Deinococcus radiodurans* R1. *Applied Environmental*
464 *Microbiology*, **66**, 2006–2011.
- 465 Freitas PS, Clarke LJ, Kennedy H, Richardson CA (2008) Inter- and intra-specimen variability
466 masks reliable temperature control on shell Mg/Ca ratios in laboratory- and field-cultured
467 *Mytilus edulis* and *Pecten maximus* (bivalvia). *Biogeosciences*, **5**, 1245-1258.
- 468 Freitas PS, Clarke LJ, Kennedy H, Richardson CA (2009). Ion microprobe assessment of the
469 heterogeneity of Mg/Ca, Sr/Ca and Mn/Ca ratios in *Pecten maximus* and *Mytilus edulis*
470 (bivalvia) shell calcite precipitated at constant temperature. *Biogeosciences*, **6**, 1209-1227.
- 471 Freitas PS, Clarke LJ, Kennedy H, Richardson CA (2016) Manganese in the shell of the bivalve
472 *Mytilus edulis*: Seawater Mn or physiological control? *Geochimica et Cosmochimica Acta*,
473 **194**, 266-278.
- 474 Frieder CA, Gonzalez JP, Levin LA (2014) Uranium in Larval Shells As a Barometer of
475 Molluscan Ocean Acidification Exposure. *Environmental Science & Technology*, **48 (11)**, 6401-
476 6408. Ganeshram RS, Francois R, Commeau J, Brown-Leger SL (2003) An experimental
477 investigation of barite formation in seawater. *Geochimica et Cosmochimica Acta*, **67**, 2599-
478 2605.
- 479 Gillikin D, Dehairs F, Lorrain A, Steenmans D, Baeyens W, Andre L (2006) Barium uptake into
480 the shells of the common mussel (*Mytilus edulis*) and the potential for estuarine paleo-
481 chemistry reconstruction. *Geochimica et Cosmochimica Acta*, **70**, 395-407.
- 482 Gillikin D, Lorrain A, Paulet YM, Andre L, Dehairs F (2008) Synchronous barium peaks in high-
483 resolution profiles of calcite and aragonite marine bivalve shells. *Geo-Marine Letters*, **28**,
484 351-358.
- 485 Gillikin D, Dehairs F (2012) Uranium in aragonitic marine bivalve shells, *Palaeogeography*,
486 *Palaeoclimatology, Palaeoecology*, **373**, doi: 10.1016/j.palaeo.2012.02.028.

- 487 Kitano Y, Oomori T (1971) The coprecipitation of uranium with calcium carbonate. *Journal of*
488 *the Oceanographic Society of Japan*, **27**, 34–42.
- 489 Klein R, Lohmann K, Thayer C (1996) Sr/Ca and C-13/C-12 ratios in skeletal calcite of *Mytilus*
490 *trossulus*: Covariation with metabolic rate, salinity, and carbon isotopic composition of
491 seawater. *Geochimica et Cosmochimica Acta*, **60**, 4207-4221.
- 492 Kleinman S, Hatcher BG, Scheibling RE, Taylor LH, Hennigar AW (1996) Shell and tissue
493 growth of juvenile sea scallops (*Placopecten magellanicus*) in suspended and bottom culture
494 in Lunenburg Bay, Nova Scotia. *Aquaculture*, **142**, 75–97.
- 495 Langmuir D (1978) Uranium mineral-solution equilibria. *Geochimica et Cosmochimica Acta*,
496 **42**, 547–569.
- 497 Lazareth CE, Vander Putten E, André L, Dehairs F (2003) High-resolution trace element
498 profiles in shells of the mangrove bivalve *Isognomon ephippium*: a record of environmental
499 spatio-temporal variations? *Estuarine, Coastal and Shelf Science*, **57**, 1103–1114.
- 500 Lazareth CE, Guzman N, Poitrasson F, Candaudap F, Ortlieb L (2007) Nyctemeral variations of
501 magnesium intake in the calcitic layer of a Chilean mollusk shell (*Concholepas concholepas*,
502 *Gastropoda*), *Geochimica et Cosmochimica Acta*, **71**, 5369-5383.
- 503 Lazareth CE, Le Cornec F, Candaudap F, Freydier R (2013) Trace element heterogeneity along
504 isochronous growth layers in bivalve shell: Consequences for environmental reconstruction.
505 *Palaeogeography, Palaeoclimatology, Palaeoecology*, **373**, 39-49.
- 506 Lazure P., Le Cann B., Bezaud M. (2018) Large diurnal bottom temperature oscillations
507 around the Saint Pierre and Miquelon archipelago. *Scientific Reports*, **8**, Article number:
508 13882.
- 509 Lorens R, Bender M (1977) Physiological Exclusion of Magnesium from *Mytilus edulis* Calcite.
510 *Nature*, **269**, 793-794.
- 511 Lorrain A, Gillikin D, Paulet YM, Chauvaud L, Le Mercier A, Navez J, André L (2005) Strong
512 kinetic effects on Sr/Ca ratios in the calcitic bivalve *Pecten maximus*. *Geology*, **33** (12), 965-
513 968.

- 514 Macaskie LE, Bonthron KM, Yong P, Goddard D (2000) Enzymatically-mediated
515 bioprecipitation of uranium by a *Citrobacter sp.*: a concerted role for extracellular
516 lipopolysaccharides and associated phosphatase in biomineral formation. *Microbiology*, **146**,
517 1855–1867.
- 518 Marali S, Schöne BR (2015) Oceanographic control on shell growth of *Arctica islandica*
519 (*Bivalvia*) in surface waters of Northeast Iceland—implications for paleoclimate
520 reconstructions. *Palaeogeography, Palaeoclimatology, Palaeoecology*, **420**, 138-149.
- 521 Min GR, Edwards RL, Taylor FW, Recy J, Gallup CD, Beck JW (1995) Annual cycles of U/Ca in
522 coral skeletons and U/Ca thermometry. *Geochimica et Cosmochimica Acta*, **59**, 2025-2042.
- 523 Mouchi V, de Rafélis M, Lartaud F, Fialin M, Verrecchia E (2013) Chemical labelling of oyster
524 shells used for time-calibrated high-resolution Mg/Ca ratios: a tool for estimation of past
525 seasonal temperature variations. *Palaeogeography, Palaeoclimatology, Palaeoecology*, **373**,
526 66–74.
- 527 Poitevin P, Thébault J, Schöne BR, Jolivet A, Lazure P, Chauvaud L (2018) Ligament, hinge,
528 and shell cross-sections of the Atlantic surfclam (*Spisula solidissima*): Promising marine
529 environmental archives in NE North America. *Plos One*, **13(6)**, e0199212.
- 530 Rosenberg GD, Hughes WW, Parker DL, Ray BD (2001) The geometry of bivalve shell
531 chemistry and mantle metabolism, *American Malacological Bulletin*, **16**, 251–261.
- 532 Schöne BR, Radermacher P, Zhang Z, Jacob DE (2013) Crystal fabrics and element impurities
533 (Sr/Ca, Mg/Ca, and Ba/Ca) in shells of *Arctica islandica*-Implications for paleoclimate
534 reconstructions. *Palaeogeography, Palaeoclimatology, Palaeoecology*, **373**, 50-59.
- 535 Shen GT, Dunbar RB (1995) Environmental controls on uranium in reef corals. *Geochimica et*
536 *Cosmochimica Acta*, **59**, 2009-2024
- 537 Shirai K, Schöne BR, Miyaji T, Radermacher P, Krause RA Jr., Tanabe K (2014) Assessment of
538 the mechanism of elemental incorporation into bivalve shells (*Arctica islandica*) based on
539 elemental distribution at the microstructural scale. *Geochimica et Cosmochimica Acta*, **126**,
540 307-320.

- 541 Stecher HA, Krantz DE, Lord CJ, Luther GW, Bock KW (1996) Profiles of strontium and barium
542 in *Mercenaria mercenaria* and *Spisula solidissima* shells. *Geochimica et Cosmochimica Acta*,
543 **60 (18)**, 3445-3456.
- 544 Stecher HA, Kogut MB (1999) Rapid Barium removal in the Delaware estuary. *Geochimica et*
545 *Cosmochimica Acta*, **63**, 1003-10012.
- 546 Surge D, Lohmann KC (2008) Evaluating Mg/Ca ratios as a temperature proxy in the
547 estuarine oyster, *Crassostrea virginica*. *Journal of Geophysical Research*, **113**, G02001.
- 548 Thébault J, Chauvaud L, L'Helguen S, Clavier J, Barats A, Jacquet S, Pecheyran C, Amouroux D
549 (2009). Barium and molybdenum records in bivalve shells: Geochemical proxies for
550 phytoplankton dynamics in coastal environments? *Limnology and Oceanography*, **54**, 1002-
551 1014.
- 552 Ullmann CV, Böhm F, Rickaby REM, Wiechert U, Korte C (2013). The Giant Pacific Oyster
553 (*Crassostrea gigas*) as a modern analog for fossil ostreoids: isotopic (Ca, O, C) and elemental
554 (Mg/Ca, Sr/Ca, Mn/Ca) proxies. *Geochemistry, Geophysics, Geosystems*, **14**, 4109–4120.
- 555 Vander Putten, E, Dehairs F, Keppens E, Baeyens W (2000) High resolution distribution of
556 trace elements in the calcite shell layer of modern *Mytilus edulis*: Environmental and
557 biological controls. *Geochimica et Cosmochimica Acta*, **64**, 997-1011.
- 558 Wanamaker AD, Kreutz KJ, Wilson T, Borns HW, Introne DS, Feindel S (2008) Experimentally
559 determined Mg/Ca and Sr/Ca ratios in juvenile bivalve calcite for *Mytilus edulis*: implications
560 for paleotemperature reconstructions. *Geo-Marine Letters*, **28**, 359-368.
- 561 Warter V, Müller W (2017) Daily growth and tidal rhythms in Miocene and modern giant
562 clams revealed via ultra-high resolution LA-ICPMS analysis - A novel methodological
563 approach towards improved sclerochemistry. *Palaeogeography, Palaeoclimatology,*
564 *Palaeoecology*, **465**, 362-375.
- 565 Witbaard R, Duineveld GCA, DeWilde PAWJ (1997) A long-term growth record derived from
566 *Arctica islandica* (Mollusca, Bivalvia) from the Fladen Ground (northern North Sea). *Journal*
567 *of the Marine Biological Association of the United Kingdom*, **77 (3)**, 801–816.

568 Yu J, Elderfield H, Jin Z, Booth L (2008) A strong temperature effect on U/Ca in planktonic
569 foraminiferal carbonates. *Geochimica et Cosmochimica Acta*, **72**, 4988–5000.

570 Zhao L, Milano S, Walliser EO, Schöne BR (2018) Bivalve shell formation in a naturally CO₂-
571 enriched habitat: Unraveling the resilience mechanisms from elemental signatures.
572 *Chemosphere*, **203**, 132-138.

Journal Pre-proof

Highlights :

- A new method to resolve shell elemental composition with a 10 μm resolution.
- Ba/Ca of *Placopecten magellanicus* shell seem to be related to phytoplankton dynamic.
- Mg/Ca and U/Ca of *P. magellanicus* shell seem partially temperature dependent.
- This species might also present a physiological control on Mg and U incorporation.
- This method may contribute to a better understanding of ion incorporation in shells.

Declaration of interests

The authors declare that they have no known competing financial interests or personal relationships that could have appeared to influence the work reported in this paper.

The authors declare the following financial interests/personal relationships which may be considered as potential competing interests: